THE UNIVERSITY of EDINBURGH

Edinburgh Research Explorer

Sustained retreat of the Pine Island Glacier

OPEN ACCESS

Sustained retreat of the Pine Island Glacier

J. W. Park,[1,2] N. Gourmelen,[3] A. Shepherd,[1] S. W. Kim,[4] D. G. Vaughan,[5] and D. J. Wingham[6]

[1] We use satellite observations to show that, between 1992 and 2011, the Pine Island Glacier hinge line retreated at a rate of 0.95 ± 0.09 km yr^{-1} despite a progressive steepening and shoaling of the glacier surface and bedrock slopes, respectively, which ought to impede retreat. The retreat has remained constant because the glacier terminus has thinned at an accelerating rate of 0.53 ± 0.15 m yr^{-2}, with comparable changes upstream. This acceleration is consistent with an intensification of ocean-driven melting in the cavity beneath the floating section of the glacier. The pattern of hinge-line retreat meanders and is concentrated in isolated regions until ice becomes locally buoyant. Because the glacier-ocean system does not appear to have reached a position of relative stability, the lower limit of sea level projections may be too conservative. **Citation:** Park, J. W., N. Gourmelen, A. Shepherd, S. W. Kim, D. G. Vaughan, and D. J. Wingham (2013), Sustained retreat of the Pine Island Glacier, *Geophys. Res. Lett.*, *40*, 2137–2142, doi:10.1002/grl.50379.

1. Introduction

[2] The West Antarctic Ice Sheet (WAIS) contains enough ice to raise eustatic sea level by over 3 m [*Bamber et al.*, 2009], and the Amundsen Sea sector of the WAIS is susceptible to accelerated retreat due the presence of a bedrock topography that lies well below sea level and deepens inland and the absence of buttressing from substantial floating ice shelf barriers [*Mercer*, 1978]. Satellite observations show that glaciers draining this sector are retreating [*Rignot*, 1998b], thinning [*Shepherd et al.*, 2001; *Shepherd et al.*, 2002; *Shepherd and Peacock*, 2003], accelerating [*Joughin et al.*, 2003], and losing mass [*Rignot*, 2008]. Observations of ice shelf thinning [*Shepherd et al.*, 2004] in the face of increased glacier discharge and a numerical simulation of glacier response to external forcing [*Payne et al.*, 2004] suggest that the surrounding ocean is the source of this imbalance. The Pine Island Glacier (PIG) is a major tributary of the WAIS Amundsen Sea sector. Satellite observations of relative tidal motion show that the PIG hinge line retreated by up to 25 km between 1992 and 2009 [*Rignot*, 1998b; *Joughin et al.*, 2010]. This retreat corresponds to a reduction in ice thickness of around 90 m at the glacier terminus considering the recent geometry [*Vaughan et al.*, 2006], a value that is consistent with direct observations of thinning acquired by satellite altimetry during the same period [*Wingham et al.*, 2009].

[3] The potential sea level contribution due to ice mass losses from the Amundsen Sea sector over the 21st century is a source of considerable uncertainty [*Meehl et al.*, 2007]. A hypothetical scaling of glacier discharge rates [*Pfeffer et al.*, 2008] indicates a potential 21st century sea level contribution in the range 4 to 15 cm from the PIG alone [*Pfeffer et al.*, 2008]. However, an extrapolation of the recent PIG volume trend acceleration [*Wingham et al.*, 2009] provides a much smaller estimated contribution of around 2 cm by the year 2100—a value that is consistent with the 1.8 cm likely estimate of a basin-scale model of the glacier response to ocean forcing [*Joughin et al.*, 2010]. Moreover, although changes occurring in the vicinity of the PIG grounding line are expected to cause thinning inland for decades to come [*Payne et al.*, 2004; *Joughin et al.*, 2003], and the presence of an extended region of lightly grounded ice at the glacier terminus has promoted rapid retreat in recent years [*Corr et al.*, 2001], the glacier and bedrock geometry farther inland impedes further retreat in numerical simulations—even allowing for an increase in ocean melting [*Joughin et al.*, 2010]. Here we use satellite radar interferometry and satellite radar altimetry to analyze the rate of hinge-line retreat and thinning to establish whether the glacier has reached this anticipated state of relative stability.

2. Methods

[4] We use interferometric synthetic aperture radar (InSAR) data acquired by the European Remote Sensing (ERS-1 and ERS-2) satellite systems to measure changes in the position of the PIG hinge line over the period 1992–2011 [*Gabriel et al.*, 1989; *Goldstein et al.*, 1993; *Rignot*, 1998a]. The InSAR data set consists of synthetic aperture radar (SAR) images recorded in 1992, 1996, 1999, 2000, and 2011 during dedicated periods when the satellites orbited in short repeat cycles. The temporal spans (baselines) of the InSAR data are 6 days (1992), 3 days (2011), and 1 day (1996, 1999, and 2000). In order to locate the glacier hinge line (the limit of tidal flexure), we subtract consecutive interferograms, corrected for the effects of topography. This procedure eliminates the signal of ice flow that is common to each individual interferogram and reveals the relative surface motion due mainly to tidal flexure of the floating glacier tongue. We then mapped the locus of the glacier hinge line at different time periods (Figure 1) by minimizing the departure between the observed tidal flexure

[1]School of Earth and Environment, University of Leeds, Leeds, UK.
[2]Department of Earth System Sciences, Yonsei University, Seoul, South Korea.
[3]Institut de Physique du Globe de Strasbourg, University of Strasbourg, Strasbourg, France.
[4]Department of Geoinformation Engineering, Sejong University, Seoul, South Korea.
[5]British Antarctic Survey, Natural Environment Research Council, Cambridge, UK.
[6]Department of Earth Sciences, University College London, London, UK.

Corresponding author: A. Shepherd, School of Earth and Environment, University of Leeds, Leeds LS2 9JT, UK. (a.shepherd@leeds.ac.uk)
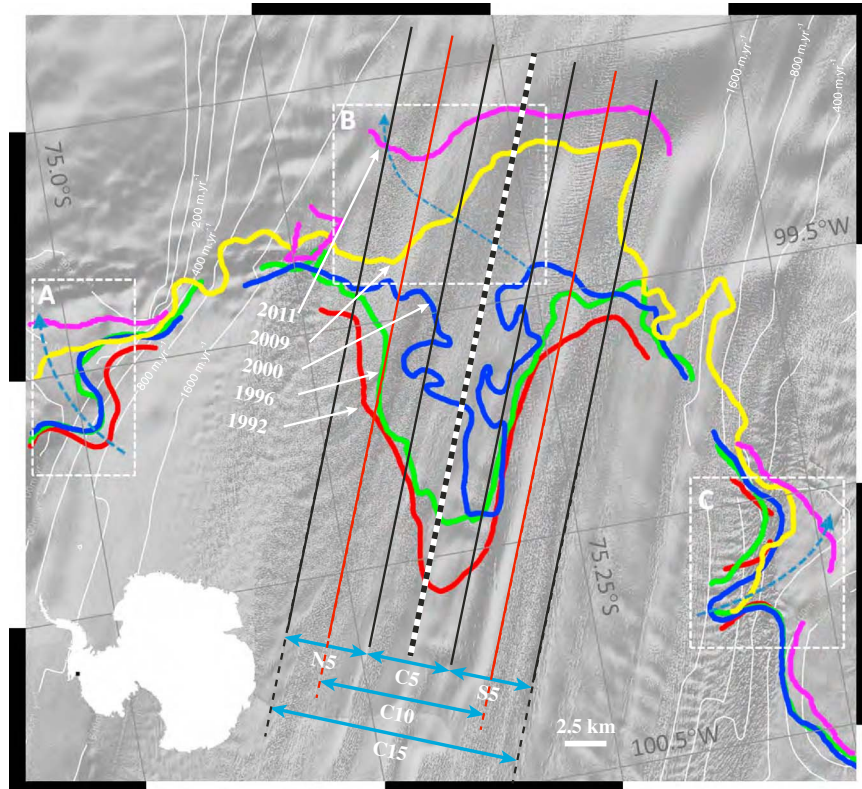
Figure 1. Hinge-line positions of the Pine Island Glacier (colored lines) superimposed on a Landsat image (gray scale). Successive hinge-line positions are marked with colored lines (red = 1992, green = 1994, blue = 2000, yellow = 2009, magenta = 2011). Thin white contours show ice velocity (m yr^{-1}). Average rates of hinge-line retreat (Table 1 and Figure 2) are calculated within the northern, central, and southern 5 km sections (N5, C5, and S5, respectively), and within the central 10 and 15 km sections (C10 and C15, respectively). Dotted line marks the profile along which the satellite radar altimeter data (Figure 3) are selected (the data are aggregated into 10 km square regions). The greatest hinge-line retreat has occurred toward the center of the fast-flowing glacier. Boxes A, B, and C highlight other regions of notable hinge-line retreat (blue dotted arrows). Rapid hinge-line retreat has occurred beyond the margins of the glacier in the vicinity of boxes A and C in recent years, despite little apparent change in the glacier surface geometry, suggesting that increased ocean melting has occurred in these regions. Rapid hinge-line retreat in the vicinity of box B has occurred, despite the apparent position of stability in 2009, due to a combination of factors; a narrow channel of lightly grounded ice has favored retreat in a northwest direction in tandem with an evolution of the ice surface slope, which has also promoted retreat.

and that of a model elastic beam. Based on the degree of data misfit to this model, as well as the tidal phase gradient in the vicinity of the hinge line, we estimate the uncertainty (1 sigma) in hinge-line position to be 0.13, 0.35, 0.51, and 0.29 km in 1992, 1996, 1999–2000, and 2011, respectively. The origin of these uncertainties lies in high-frequency noise of the InSAR measurement; we do not observe a systematic long-wavelength misfit that could indicate a departure of the observed flexure from the elastic beam model assumption that is commonly used to locate hinge-line positions [*Vaughan*, 1995; *Rignot*, 1998a].

[5] Since 1992, the PIG hinge line has retreated by as much as 28.4 km along the central section of flow (Figure 1). However, the degree of hinge-line migration has varied in space and time—in some places by as little as 9.5 km—and so we computed the average rate of hinge-line retreat within different regions of the grounding zone (Table 1). In the first instance, we calculated the rate of hinge-line retreat along three adjacent 5 km wide sections spanning northern (N5), central (C5), and southern (S5) portions of the glacier trunk (Figure 1) to provide a detailed picture of how the migration has occurred over time. We also calculated the rate

of hinge-line retreat along a 10 km wide central section (C10, Figure 1) of the glacier to facilitate a comparison with satellite altimeter observations aggregated over a similar area [*Shepherd and Peacock*, 2003]. The average rate of hinge-line retreat is computed as the reduction in grounded area between successive hinge-line positions, divided by the section width perpendicular to the direction of ice flow. On average, an area of 14.2 ± 1.3 km^2 has become ungrounded each year (Figure 2a).

[6] The PIG hinge-line position migrates due to changes in ice thickness because it rests close to a state of hydrostatic balance [*Thomas and Bentley*, 1978; *Rignot*, 1998b]. We used this relationship to calculate the rate of ice thinning associated with hinge-line retreat from the InSAR data set. The change in ice thickness over an intervening time period $\dot{h}$ h (positive for thickening) is given by

$$\dot{h} = \left(\frac{\rho_w}{\rho_i}\right)\dot{z} - \left[\alpha - \beta\left(1 - \frac{\rho_w}{\rho_i}\right)\right]\dot{x} \qquad (1)$$

where z is the change in ocean tide, $\dot{x}$ (positive for retreat) is the change in hinge-line position, ρ_w is the density of

Table 1. Retreat Rate of the PIG Hinge Line Along Parallel Sections of the Glacier Breadth (See Figure 1)[a]

	Northern 5 km, N5 (km yr^{-1})	Central 5 km, C5 (km yr^{-1})	Southern 5 km, S5 (km yr^{-1})	Central 10 km, C10 (km yr^{-1})	Central 15 km, C15 (km yr^{-1})
1992–1996	0.48 + 0.24	0.75 + 0.17	0.64 + 0.27	0.67 + 0.22	0.63 + 0.23
1996–2000	1.21 + 0.23	1.00 + 0.21	0.54 + 0.26	1.36 + 0.23	0.92 + 0.23
2000–2009[a]	0.35 + 0.13	1.37 + 0.15	0.80 + 0.16	1.21 + 0.15	0.84 + 0.15
2009[a]–2011	2.81 + 0.72	1.23 + 0.78	1.32 + 0.81	1.53 + 0.87	1.79 + 0.87
2000–2011	0.79 + 0.09	1.33 + 0.12	0.89 + 0.13	1.26 + 0.09	1.00 + 0.09

[a]Using the hinge line located in 2009 with coarse-resolution speckle-tracked range offsets [*Joughin et al.*, 2010].

seawater = 1027.5 kg m^{-3} [*Jacobs et al.*, 1996], ρ_i is the density of ice = 900 kg m^{-3} [*Jenkins et al.*, 1997], and α and β are the slopes of the ice surface and base, respectively. The local balance between surface and basal slopes governs the rate of hinge-line migration for a given change in ice thickness. Repeat observations of ice surface elevation [e.g. *Wingham et al.*, 2009] suggest that the surface slope in the vicinity of the PIG hinge line has altered considerably over time. To account for this variation, we estimate α averaged between the locations of successive hinge-line positions using

(A)

a sequence of glacier surface slopes generated from satellite and airborne data [*Bamber and Bindschadler*, 1997; *DiMarzio et al.*, 2007; *Krabill*, 2011], and we estimate β using a model of the bedrock elevation [*Vaughan et al.*, 2006]. In the absence of direct observations, we use a model of Antarctic ocean tide (an updated version of the regional inverse model described by *Padman et al.* [2002]) to assess the fluctuation in grounding line position due to tidal displacement. However, because tide models tend to perform least well when predicting tidal phase [*Shepherd and Peacock*, 2003], we estimate the uncertainty associated with z using the maximum modeled tidal range in the vicinity of the PIG (1.8 m) following a conservative approach [*Rignot*, 1998a] and by taking account of variability in the basal slope [*Bindschadler et al.*, 2011]. Using these assumptions, we determined the rates of ice thickness change in the vicinity of the PIG grounding line over the survey period (Figure 2b) associated with the observed hinge-line retreat.

[7] We obtained additional estimates of ice thickness changes inland of the PIG hinge line from repeat-pass satellite radar altimeter data. For this exercise, we processed a continuous record of data acquired by the ERS-1, ERS-2, and ENVISAT satellite radar altimeters between 1994 and 2010. Time series of surface elevation change were developed at crossing points of the satellites' ground tracks falling within the PIG drainage basin during 35 day orbit repeat mission phases, using the method of dual-cycle crossovers [*Zwally et al.*, 1989]. Elevation measurements were corrected for the lag of the leading edge tracker, surface scattering variation, dry atmospheric mass, water vapour, the ionosphere, solid Earth tide, and ocean loading tide [*Wingham et al.*, 1998; *Shepherd et al.*, 2001; *Wingham et al.*, 2009]. To cross-calibrate the observations recorded by successive satellites, we corrected for the differences between the average elevation changes occurring during periods of mission overlap. At each crossing point, we formed a time series of elevation change, and these data were then aggregated into 10 km × 10 km grid cells to accommodate temporal variations in the location of satellite orbits [*Shepherd and Peacock*, 2003]. For each grid cell, we computed the average rate of elevation change during discrete time periods (e.g., Figure 3), and we estimated the error associated with each time series according to the variance of the data.

3. Results

[8] Although rates of hinge-line retreat have been high near to the center of the PIG, they diminish rapidly toward the glacier margins. Between 1992 and 2010, the spatially averaged rate of hinge-line retreat within the central 15 km of the glacier (C15, Figure 1) has remained broadly constant at 0.95 ± 0.09 km yr^{-1} (Table 1). However, there have been also considerable temporal variations in the hinge-line retreat
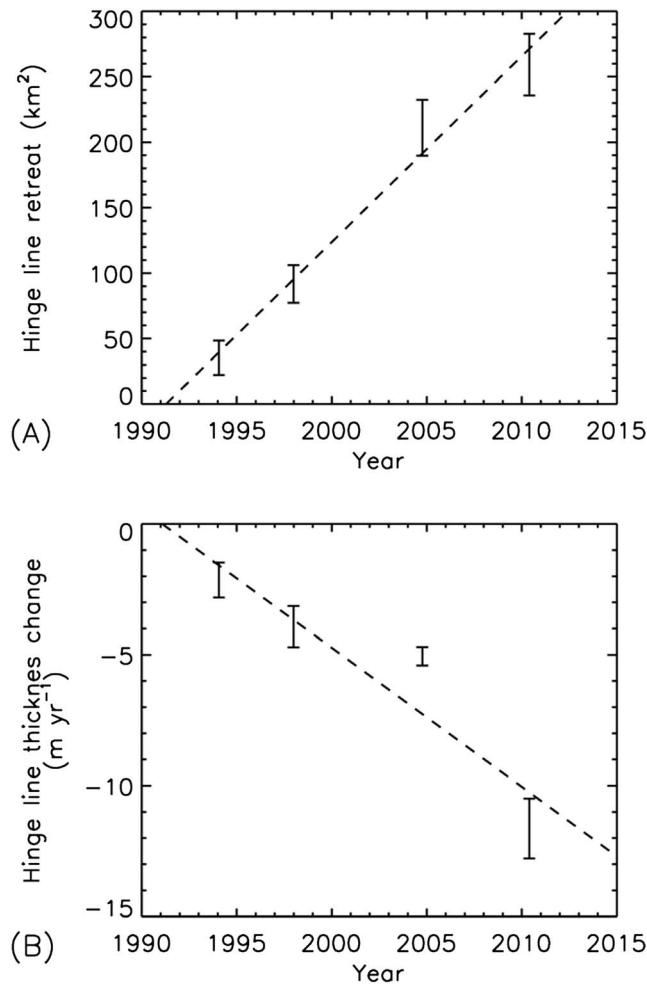

(B)

Figure 2. (a) Retreat and (b) ice thickness change at the hinge line of the Pine Island Glacier. Retreat area is computed within the central 15 km of the glacier (see Figure 1) to capture the entire signal. Dashed lines are linear regressions of retreat and ice thickness change. Thickness changes are computed within the central 10 km for ease of comparison with satellite altimeter data (Figure 3).
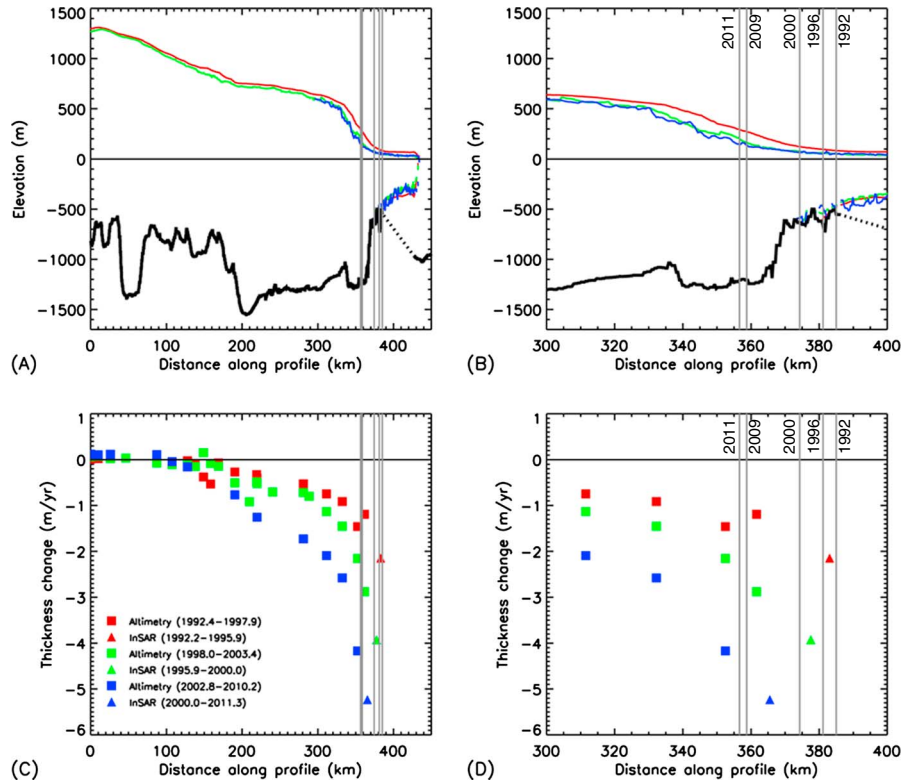
Figure 3. (a, b) Geometry and (c, d) rate of ice thickness change along a profile of the Pine Island Glacier (see Figure 1) during three time intervals. Thickness changes are determined using either satellite altimetry (squares) or satellite InSAR (triangles). Vertical gray lines chart migrating glacier hinge-line position which, since 2009, has been situated in a location where the bedrock has shoaled.

rate over the course of our survey, with episodes of rapid and asymmetric migration. During the periods 1992–2000, 2000–2009, and 2009–2011, for example, hinge-line retreat was concentrated within the central, southern, and northern sections of the PIG, respectively. The largest measured rate of hinge-line retreat (2.8 ± 0.7 km yr^{-1}) occurred within the northernmost 5 km wide section of the PIG during the most recent period captured by our InSAR data (2009–2011). These irregular patterns can be explained in part by the limiting influence of the glacier geometry. For a constant rate of ice thinning, for example, the degree of hinge-line retreat is dependent upon the surface and bedrock slopes which vary in space and, in the case of the ice surface, over time.

[9] The PIG bedrock and surface slopes shoal and steepen inland of the 1992 hinge-line position, respectively (Figure 3a), and this geometry tends to impede retreat [see equation (1)]. As a consequence, the near-constant rate of hinge-line retreat during our survey must reflect an accelerated rate of ice thinning (Figure 2b). Within the central 10 km of the PIG, the rate of ice thinning associated with hinge-line retreat has progressively increased from 2.1 ± 0.7 m yr^{-1} between 1992 and 1996 to 11.6 ± 1.1 m yr^{-1} between 2009 and 2011. According to the InSAR data, the average rate of ice thinning at the PIG hinge line has accelerated by 0.53 ± 0.15 m yr^{-2} over the 19 year survey period.

[10] We compared rates of hinge-line ice thinning determined from the InSAR data set with those determined farther inland using satellite radar altimetry. According to the altimeter data set, ice thinning is observed to start around 200–250 km inland and increase sharply toward the PIG

hinge line (Figure 3). To facilitate a more detailed comparison, we estimated rates of ice thinning during successive time periods when the respective data sets were coincident (1992–1998, 1998–2003, and 2000–2010). These periods were selected to optimize the degree of temporal overlap, the duration of the altimeter data, and the provenance of the altimeter data in relation to the three satellite platforms. Rates of ice thinning determined from InSAR along the central 10 km of the PIG are consistent with those determined from altimetry (Figure 3), illustrating that the independent techniques are complementary. Along a streamwise profile of the PIG, temporally averaged thinning rates are greater at the hinge line (as determined by InSAR) by a proportion that is consistent with the rate of increase farther inland (as determined by altimetry). Given their complementary nature, the InSAR data may prove useful in determining ice volume changes in regions that are beyond the locus of the altimeter measurements.

4. Discussion

[11] The rate of hinge-line retreat we have recorded may be compared with that determined during the overlapping periods of previous surveys [*Rignot*, 1998b, 2002; *Joughin et al.*, 2010]. For example, average retreat rates of 0.64 and 0.55 km yr^{-1} have been estimated across a 14 km wide center profile [*Rignot*, 1998b] during the periods 1992–1996 and 1996–2000, respectively, as compared to our estimated retreat rates of 0.63 ± 0.23 and 0.92 ± 0.23 km yr^{-1} across a partially overlapping 15 km wide profile.

The hinge-line position we have recorded in the year 2000 is, however, considerably less regular than that of a previous survey [*Rignot*, 2002], showing greater retreat to the south of the glacier centerline. When compared to the 2009 hinge-line position located using the technique of radar speckle tracking [*Joughin et al.*, 2010], which has coarse resolution, the 2011 location is between 2 and 5 km farther inland—more than double the average rate of retreat since 1992 (Table 1). The hinge-line positions are irregularly shaped, and retreat within the central portion of the glacier has been asymmetrical at all times. Rapid migration tends to occur along relatively confined sections of the hinge line. Prior to 2009, for example, steep surface slopes to the north of the PIG hinge line presented an obstacle to retreat in that sector (Figure 1). Since then, the hinge line has retreated across a submarine bedrock ridge (see Figure 3b), and the principal trajectory of retreat has been northward and inland, eroding a grounded promontory that was present in 2009.

[12] Accelerated thinning and retreat of ice at the Pine Island Glacier grounding line has occurred in the face of well-documented increases in the rate of glacier discharge [*Rignot*, 2008], which should thicken the floating section through advection. Although additional grounding line retreat may result from creep thinning associated with altered ice stream dynamics [*Thomas et al.*, 2011], our observations of accelerated thinning are consistent with measurements of changing oceanographic conditions at the glacier terminus over the period 1994–2009 [*Jacobs et al.*, 2011]. These oceanographic data reveal strengthening circulation in an enlarged sub–ice shelf cavity, leading to faster ice melting. The emergence of an enlarged ocean cavity has resulted in part from retreat of the glacier across a submarine bank upon which it was formerly grounded [*Jenkins et al.*, 2010], allowing relatively warm (~4°C above freezing) seawater to access the glacier grounding line.

[13] The shoaling of the PIG in the vicinity of the 2011 hinge line does not favor retreat, and further retreat is at odds with simulations of the glacier evolution under conditions of increased ocean melting [*Joughin et al.*, 2010]. However, the PIG geometry has impeded retreat at other times during our survey, and yet the retreat has progressed over time. Moreover, recent simulations of the PIG evolution that utilizes an adaptive-resolution domain [*Gladstone et al.*, 2012; *Cornford et al.*, 2013] have suggested that the grounding line may be able to retreat much farther inland should ocean melting persist. It is also possible that ocean melting has exceeded that imposed during existing simulations. The progressive retreat of the PIG hinge line has occurred presumably as a result of changes in both the rate of ocean melting and the glacier surface slope, the latter occurring as a dynamical response to reduced grounding [*Joughin et al.*, 2003; *Payne et al.*, 2004]. Although a substantial bedrock peak occurs around 25 km inland of the present hinge-line position (Figure 3d), this feature does not straddle the entire glacier width [*Vaughan et al.*, 2006], and relief to the south side of the glacier, in particular, slopes gently. However, although the hinge line has retreated since 2009, analysis of glacier velocities reveals that the glacier speed has yet to increase (I. Joughin, personal communication), which suggests that further dynamical imbalance has yet to occur.

5. Conclusions

[14] Even though the Pine Island Glacier hinge line has now migrated into the bedrock trough within which the main trunk of the glacier is seated, where basal slopes shoal and impede retreat, it is now retreating at a faster mean rate $(1.8 \pm 0.9 \text{ km yr}^{-1})$ than at any time since it has been first located (Table 1). This observation may have important implications for projections of future mass losses from the glacier [*Rignot et al.*, 2011] and the associated global sea level contribution. The wide range of current sea level projections (2–14 cm by the year 2100) is bounded, at the lower end, by the results of a coupled ice-ocean interaction model of the glacier response to modest ocean forcing [*Joughin et al.*, 2010] and, at the upper end, by the results of a hypothetical assessment of ice mass losses under a heuristic scaling of the present-day imbalance [*Pfeffer et al.*, 2008]. Our observations of accelerated thinning and ongoing rapid hinge-line retreat, coupled with the observed strengthening of ocean melting within the sub–ice shelf cavity [*Jacobs et al.*, 2011], suggest that the lower limit may be found on a conservative forcing scenario. An accurate projection of the glacier response to climate forcing will need to capture details of how the ocean circulates within the sub–ice shelf cavity and how it interacts with the ice shelf base.

References

Bamber, J. L., and R. A. Bindschadler (1997), An improved elevation dataset for climate and ice-sheet modelling: Validation with satellite imagery, *Ann. Glaciol.*, *25*, 439–444.

Bamber, J. L., R. E. M. Riva, B. L. A. Vermeersen, and A. M. LeBrocq (2009), Reassessment of the potential sea-level rise from a collapse of the West Antarctic Ice Sheet, *Science*, *324*, 901–903, doi:10.1126/science.1169335.

Bindschadler, R., et al. (2011), Getting around Antarctica: New high-resolution mappings of the grounded and freely-floating boundaries of the Antarctic Ice Sheet created for the International Polar Year, *Cryosphere Discuss.*, *5*, 183–227, doi:10.5194/tcd-5-183-2011.

Cornford, S. L., D. F. Martin, D. T. Graves, D. F. Ranken, A. M. Le Brocq, R. M. Gladstone, A. J. Payne, E. G. Ng, and W. H. Lipscomb (2013), Adaptive mesh, finite volume modeling of marine ice sheets, *J. Comput. Phys. 232* (1), 529–549, doi:10.1016/j.jcp.2012.08.037.

Corr, H. F. J., C. S. M. Doake, A. Jenkins, and D. G. Vaughan (2001), Investigations of an "ice plain" in the mouth of Pine Island Glacier, Antarctica, *J. Glaciol.*, *47*(156), 51.

DiMarzio, J. P., A. Brenner, R. Schutz, C. A. Shuman, and H. J. Zwally (2007), GLAS/ICESat 500 m Laser Altimetry Digital Elevation Model of Antarctica, digital media, Natl. Snow and Ice Data Cent., Boulder, Colo.

Gabriel, A. K., R. M. Goldstein, and H. A. Zebker (1989), Mapping small elevation changes over large areas—Differential radar interferometry, *J. Geophys. Res.*, *94*(B7), 9183–9191.

Gladstone, R. M., et al. (2012), Calibrated prediction of Pine Island Glacier retreat during the 21st and 22nd centuries with a coupled flowline model, *Earth Planet. Sci. Lett. 333–334*, 191–199, doi:10.1016/j.epsl.2012.04.022.

Goldstein, R. M., H. Engelhardt, B. Kamb, and R. M. Frolich (1993), Interferometry for monitoring ice-sheet motion—Application to an Antarctic ice stream, *Science*, *262*(5139), 1525.

Jacobs, S. S., H. H. Hellmer, and A. Jenkins (1996), Antarctic ice sheet melting in the Southeast Pacific, *Geophys. Res. Lett.*, *23*(9), 957.

Jacobs, S. S., A. Jenkins, C. F. Giulivi, and P. Dutrieux (2011), Stronger ocean circulation and increased melting under Pine Island Glacier ice shelf, *Nat. Geosci.*, *4*, 519, doi:10.1038/ngeo1188.

Jenkins, A., D. G. Vaughan, S. S. Jacobs, H. H. Hellmer, and J. R. Keys (1997), Glaciological and oceanographic evidence of high melt rates beneath the Pine Island Glacier, West Antarctica, *J. Glaciol.*, *43*(143), 114.

Jenkins, A., P. Dutrieux, S. S. Jacobs, S. D. McPhail, J. R. Perrett, A. T. Webb, and D. White (2010), Observations beneath Pine Island Glacier in West Antarctica and implications for its retreat, *Nat. Geosci.*, *3*(7), 468–472, doi:10.1038/ngeo890.

Joughin, I., E. Rignot, C. E. Rosanova, B. K. Lucchitta, and J. Bohlander (2003), Timing of recent accelerations of Pine Island Glacier, Antarctica, *Geophys. Res. Lett. 30*(13), 1706, doi:10.1029/2003GL017609.

Joughin, I., B. E. Smith, and D. M. Holland (2010), Sensitivity of 21st century sea level to ocean induced thinning of Pine Island Glacier, Antarctica, *Geophys. Res. Lett. 32*, L20502, doi:10.1029/2010GL044819.

Krabill, W. B. (2011), *IceBridge ATM L2 Ice Elevation, Slope, and Roughness*, digital media, Natl. Snow and Ice Data Cent., Boulder, Colo.

Meehl, G. A., et al. (2007), Global Climate Projections. in *Climate Change 2007: The Physical Science Basis. Contribution of Working Group I to the Fourth Assessment Report of the Intergovernmental Panel on Climate Change*, edited by S. Solomon, Qin, D., M. Manning, Z. Chen, M. Marquis, K. B. Averyt, M. Tignor, and H. L. Miller, Cambridge Univ. Press, Cambridge, U. K

Mercer, J. H. (1978), West Antarctic Ice sheet and CO_2 greenhouse effect: A threat of disaster, *Nature*, *271*, 321–325.

Padman, L., H. A. Fricker, R. Coleman, S. Howard, and L. Erofeeva (2002), A new tide model for the Antarctic ice shelves and seas, *Ann. Glaciol.*, *34*, 247–254, doi:10.3189/172756402781817752.

Payne, A. J., A. Vieli, A. Shepherd, D. J. Wingham, and E. Rignot (2004), Recent dramatic thinning of largest West Antarctic ice stream triggered by oceans, *Geophys. Res. Lett. 31*(23), L23401, doi:10.1029/2004GL021284.

Pfeffer, W. T., J. T. Harper, and S. O'Neel (2008), Kinematic constraints on glacier contributions to 21st-century sea-level rise, *Science*, *321*, 1340–1343, doi:10.1126/science.1159099.

Rignot, E. (1998a), Hinge-line migration of Petermann Gletscher, north Greenland, detected using satellite-radar interferometry, *J. Glaciol.*, *44*, 469–476.

Rignot, E. J. (1998b), Fast recession of a West Antarctic glacier, *Science*, *281*(5376), 549.

Rignot, E. (2002), Ice-shelf changes in Pine Island Bay, Antarctica, 1947–2000, *J. Glaciol.*, *48*(161), 247–256, doi:10.3189/172756502781831386.

Rignot, E. (2008), Changes in West Antarctic ice stream dynamics observed with ALOS PALSAR data, *Geophys. Res. Lett.*, *35*, L12505, doi:10.1029/2008GL033365.

Rignot, E., I. Velicogna, M. R. van den Broeke, A. Monaghan, and J. Lenaerts (2011), acceleration of the contribution of the Greenland and Antarctic ice sheets to sea level rise, *Geophys. Res. Lett.*, *38*, L05503, doi:10.1029/2011GL046583.

Shepherd A., and N. R. Peacock (2003), Ice shelf tidal motion derived from ERS altimetry, *J. Geophys. Res.*, *108*(C6), 3198, doi:10.1029/2001JC001152.

Shepherd, A., D. J. Wingham, J. A. D. Mansley, and H. F. J. Corr (2001), Inland thinning of Pine Island Glacier, West Antarctica, *Science*, *291*(5505), 862.

Shepherd, A., D. J. Wingham, J. A. D. Mansley, (2002), Inland thinning of Amundsen Sea sector, West Antarctica, *Geophys. Res. Lett.*, *29*, 1364, doi:10.1029/2001GL014183.

Shepherd, A., D. Wingham, and E. Rignot (2004), Warm ocean is eroding West Antarctic Ice Sheet, *Geophys. Res. Lett. 31*(23), L23402, doi:10.1029/2004GL021106.

Thomas, R. H., and C. R. Bentley (1978), A model for Holocene Retreat of the West Antarctic Ice Sheet, *Quat. Res.*, *10*, 150.

Thomas, R., E. Frederick, J. Li, W. Krabill, S. Manizade, J. Paden, J. Sonntag, R. Swift, and J. Yungel (2011), Accelerating ice loss from the fastest Greenland and Antarctic glaciers, *Geophys. Res. Lett.*, *38*, L10502, doi:10.1029/2011GL047304.

Vaughan, D. G. (1995), Tidal flexure at ice shelf margins, *J. Geophys. Res.*, *100*, 6213–6224.

Vaughan, D. G. et al. (2006), New boundary conditions for the West Antarctic Ice sheet: Subglacial topography beneath Pine Island Glacier, *Geophys. Res. Lett.*, *33*, L09502, doi:10.1029/2005GL025561.

Wingham, D. J., A. J. Ridout, R. Scharroo, R. J. Arthern, and C. K. Shum (1998), Antarctic elevation change from 1992 to 1996, *Science*, *282*(5388), 456–458.

Wingham, D. J., D. W. Wallis, and A. Shepherd (2009), Spatial and temporal evolution of Pine Island Glacier thinning, 1995–2006, *Geophys. Res. Lett.*, *36*, L17501, doi:10.1029/2009GL039126.

Zwally, H. J., A. C. Brenner, J. A. Major, R. A. Bindschadler, and J. G. Marsh (1989), Growth of Greenland Ice Sheet—Measurement, *Science*, *246*(4937), 1587.